Journal of Magnetic Resonance Open 10-11 (2022) 100051

Contents lists available at ScienceDirect

Journal of Magnetic Resonance Open

journal homepage: www.sciencedirect.com/journal/journal-of-magnetic-resonance-open

Chemical shielding and electric field gradient tensors of disodium 5′-adenosine triphosphate trihydrate determined by solid-state NMR spectroscopy and *ab initio* calculations

Gurpreet Singh [a], Usha D. Phalgune [a], Perunthiruthy K. Madhu [b,*], Niels Chr. Nielsen [c,*], Subramanian Ganapathy [a,*]

[a] *Central NMR Facility, National Chemical Laboratory, Dr. Homi Bhabha Road, Pune 411008, India*
[b] *Tata Institute of Fundamental Research Hyderabad, Survey No.36/P, Gopanapally Village, Serilingampally Mandal, Ranga Reddy Dist. Hyderabad 500 046, India*
[c] *Center for Insoluble Protein Structures (inSPIN), Interdisciplinar Nanoscience Center (iNANO) and Department of Chemistry, University of Aarhus, Gustav Wieds Vej 14, DK-8000 Aarhus C, Denmark*

ARTICLE INFO

Keywords:
Nucleotide
Adenosine triphosphate
Solid-state NMR
Interaction tensors
ab initio calculations

ABSTRACT

The tri-phosphate and sodium ion environments in well crystallized disodium 5′adenosine triphosphate trihydrate (ATP•3H_2O) are investigated using high-resolution solid-state NMR spectroscopy and *ab initio* calculations. The six inequivalent phosphorus sites resolved in ^{31}P MAS spectra have been assigned on the basis of experimentally obtained results and theoretical *ab initio* quantum chemical calculations of ^{31}P chemical shielding tensors with increased numerical accuracy. Aided by ^{31}P-^{31}P dipolar connectivity established in DQ-SQ correlation experiment and DFT calculations carried out at the B3LYP/(aug-cc-pDVZ(3s,2p,1d), 6–31G(d,p)) level, phosphorus resonance assignments in MAS spectra have been made and the ^{31}P chemical shielding anisotropies and tensor orientations in the molecule-fixed frame have been determined. ^{31}P shielding tensors are found to be oriented with the most shielded direction nearly perpendicular to the O-P-O plane involving the two adjoining oxygens. The complete resolution of the four sodium sites has been achieved from 3Q-MAS experiments performed at 7.05 T and this has enabled ^{23}Na quadrupole parameters to be determined experimentally and compared with theoretical calculations. Besides aiding a partial resonance assignment of the ^{23}Na 3Q-MAS spectrum, our HF/6–311++*G*(2d,2p) calculations of ^{23}Na EFG tensors show that for two sodium sites which are tightly coordinated the orientation of the EFG tensor is distinct. These exhibit unique directions along which the field gradient is the smallest and largest.

Introduction

Adenosine tri-phosphate (ATP), a nucleotide of great fundamental importance, plays many significant roles in chemical energy storage and energy transfer. It was first formulated as a derivative of adenosine 5-phosphate containing three phosphoric acid groups[1] and was synthesized in the laboratory [2]. Considering the key biological functions played by nucleotides in the metabolism of living organisms, the study of conformational changes exhibited by Na_2ATP crystals[3] was of considerable early interest since it led to the development of a basic model for understanding the induced fitting of ATP in ATP-enzyme complexes. Besides, the structural information gathered in the crystalline state became valuable for understanding the ATP-protein interactions.

The structure of ATP(5′)Na_2•3H_2O was first determined by Kennard *et a1* [4]. using single crystal X-ray diffraction. This structure was further refined in a later work [5]. Sugawara *et al.* [6]. showed that Na_2ATP crystallizes in two forms, namely, dihydrate and trihydrate, depending on the humidity conditions existing during crystallization. Na_2ATP undergoes a reversible humidity controlled structural transition between its dihydrate and trihydrate forms [6–8]. Both the crystal forms are orthorhombic belonging to the space group $P2_12_12_1$ and there is a change in unit cell parameters due to the crystal transition (ESI: Table S1). An interesting feature revealed by the X-ray studies is the existence of the ATP molecule as a dimer for both the hydrate forms. However, the two forms show marked differences, especially for one of

* Corresponding authors.
E-mail addresses: madhu@tifrh.res.in (P.K. Madhu), ncn@chem.au.dk (N.Chr. Nielsen), saras.ganapathy@gmail.com (S. Ganapathy).

https://doi.org/10.1016/j.jmro.2022.100051
Received 8 December 2021; Received in revised form 3 March 2022; Accepted 9 March 2022
Available online 16 March 2022

the dimer molecules, in hydrogen bonding, sugar puckering and the conformation of the exocyclic group around P-O ester bond. Importantly, the work of Sugawara *et al*[6] indicated that for ATP(5′)Na_2•$3H_2O$ the assignments of one of the sodiums (Na4) and water oxygen (OW4) must be interchanged. Our studies conform to the crystal structure data[6] of ATP(5′)Na_2•$3H_2O$, which affords a structure-based assignment of the solid-state NMR data and also provides the opportunity to determine parameters for the anisotropic ^{31}P chemical shielding tensor and the ^{23}Na electric field gradients by *ab initio* calculations with improved numerical accuracy. The asymmetric unit of ATP(5′)Na_2•$3H_2O$ and the packing diagram are shown in Figure S1 (ESI).

In the context of the biological significance of ATP and the structural characteristics that it is endowed with, difficulties are encountered in obtaining the structurally stable crystalline form conforming to a specific hydrate (di- or tri-hydrate). This is due to the humidity controlled structural transformation[6–8] as mentioned above, which necessitates crystallization of ATP at the desired and well controlled humidity during the crystallization process. For the ATP trihydrate, once well crystallized and prepared, the various non-equivalent ^{31}P sites, arising due to crystallographic causes, can be resolved in ^{31}P MAS spectra and the chemical shielding anisotropy parameters can be retrieved by solid-state NMR methods. For the dimeric ATP(5′)Na_2•$3H_2O$ structure, the information about the phosphate group binding to the metal, which is lost due to ion exchange in liquid state, can be gleaned from solid-state NMR experiments. The anisotropy of ^{31}P chemical shielding can be determined and assigned to specific phosphorus sites in the molecule. Similarly, the electric field gradients (EFG) for the sodium sites can be determined in a rigid lattice. However, it is essential that no structural transformation occurs during any of the ^{31}P and ^{23}Na experimental measurements so that the solid-state NMR based structural characterization essentially conforms to the trihydrate form.

There are previously reported studies of ATP•$3H_2O$ both by experimental solid-state NMR and quantum chemical calculations [9–11]. Potrzebowski *et al.* [11]. used ^{31}P double-quantum (DQ) experiments for semi-quantitative measurement of ^{31}P-^{31}P internuclear distances but no phosphorus site assignments for the ATP dimer structure was made in this study. The other two studies[9,10] of ATP deal with ^{23}Na site identification by MQ-MAS. Although four sodium sites were identified in these studies, their complete structure based assignment and precise characterization in terms of EFG tensors have remained incomplete[10] and uncertain[9], the latter attributable to the lower basis set [6–31G (d)] used in the quantum chemical calculations[9] at which the EFG results do not seem to have converged.

In the present work, we have studied one of the well crystallized hydrate forms of ATP, namely, ATP(5′)Na_2•$3H_2O$, which remains structurally stable as a trihydrate and there exists no admixture of the two hydrate forms (di- and tri-) at any time. This has ensured a one-to-one correspondence between the solid-state NMR results that we have obtained and the X-ray structure reported by Sugawara *et al.* [6]. Accordingly, we have determined the ^{31}P chemical shielding and ^{23}Na EFG tensors of ATP(5′)Na_2•$3H_2O$ by high resolution ^{31}P and ^{23}Na solid-state NMR spectroscopy and *ab initio* calculations. For the various phosphorus sites, resolved at their isotropic chemical shifts by MAS, ^{31}P 2D magic angle turning (MAT) [12], under ^{1}H-^{31}P cross-polarization, we have determined the chemical shielding tensors for all the non-equivalent phosphorus sites in the dimer molecule. Further, through dipolar decoupled MQ-MAS[13] experiments performed at 7.05 T, which serves to enhance the signal resolution along the isotropic dimension and the quadrupolar second-order effects along the MAS dimension, we have completely resolved the non-equivalent sodium sites and determined the chemical shielding and electric field gradient parameters for the four sodium sites in the dimer structure of ATP(5′)Na_2•$3H_2O$.

We have additionally carried out *ab initio* calculations of the ^{31}P chemical shielding and ^{23}Na EFG tensors using a dimer cluster model derived using positional coordinates with correct sodium assignments as reported in the X-ray structure by Sugawara et al. [6]. The improved numerical accuracy in final results, due to the astute choice of basis sets employed for ^{31}P shielding (B3LYP/(aug-cc-pDVZ(3s,2p,1d), 6–31G(d,p)) and ^{23}Na EFG (HF/6–311++G(2d,2p)) calculations, have enabled the signal assignments in MAS/MQ-MAS spectra. Furthermore, the orientation of the ^{31}P shielding tensor at each phosphorus site could be determined and the triphosphate conformation ascertained. Likewise, the Na metal environments could be fully characterized by their associated chemical shift (δ_{CS}) and quadrupolar coupling ($C_Q = e^2qQ/h$, η_Q) interaction parameters which are experimentally derived from simulations of MAS/MQ-MAS spectra.

Our studies have also provided the first opportunity to study the phosphorus and sodium environments in a single study on a well crystallized sample of ATP(5′)Na_2•$3H_2O$ under identical sample and experimental conditions, paving the way for ^{31}P and ^{23}Na resonance assignments in ^{1}H-^{31}P CP-MAS and ^{23}Na triple-quantum magic-angle-spinning (3Q-MAS) spectra, respectively. Besides, theoretical determination of ^{31}P chemical shielding and ^{23}Na EFG tensors with improved numerical accuracy has been afforded in our study. *Prima facie*, our calculations are based on dimer cluster models of ATP(5′)Na_2•$3H_2O$ which were built using correct sodium assignments in the structure and the more accurately determined atomic coordinates reported by Sugawara et al. [6]. This removes the structural ambiguity that arises due to the conflicting atomic assignment (Na4 and OW2) in the original X-ray structure on which the previously reported calculations[9,11] seem to have been based.

Materials and methods

Crystallization of ATP(5′)Na_2•$3H_2O$

A near-saturated solution of the commercially available Na_2ATP (Sigma-Aldrich) was prepared by adding an equal volume of dioxane to the hot aqueous solution. This solution was set aside at a constant temperature of 20°C for a period of four days. Seeds so formed were then allowed to grow further over a period of three weeks at controlled humidity to yield sufficient quantity of material for the NMR experiments. The crystals were finally filtered, dried and packed into a 4 mm zirconia rotor. Care was taken to ensure that it remained in trihydrate form during the NMR measurements by quickly transferring to the MAS rotor and sealing the sample with a very tight fit KEL-F cap. It was confirmed that the sample conforms to the trihydrate form by recording ^{31}P and ^{13}CP-MAS spectra during the entire course of our experimentation over several months and comparing them with those reported by Shindo *et al* [8] for the trihydrate form (ESI: Fig. S2).

Solid-state NMR spectroscopy

^{31}P solid-state NMR experiments were performed at ambient probe temperature (23°C) on wide-bore Bruker Avance-II 300 and DRX-500 NMR spectrometers, the latter equipped with a solid-state CP-MAS accessory. Variable speed (4 – 13.5 kHz) ^{31}P CP-MAS and 2D MAT experiments were carried out at 202.454 MHz on the 500 MHz instrument using a 4 mm ^{1}H-BB CP-MAS probe head. ^{31}P DQ and ^{23}Na 3Q-MAS experiments were performed at 121.4422 and 79.3557 MHz, respectively, on the solids 300 MHz spectrometer equipped with three RF channels and 1 kW amplifier. Lower B_0 field (7.01 T) was preferred for ^{23}Na experiments due to the increased quadrupole effects along the isotropic and MAS dimensions in 3Q-MAS spectra. 2D MAT experiments employed the PHORMAT pulse sequence[14] incorporating cross-polarization at the beginning of the sequence. Sample spinning was maintained at 4000 Hz. Typically 320 t_1 incrementswere used with a dwell time of 36 μs and 64 transients, were collected each time with a recycle delay of 4 s. The 2D ^{31}P through-space double-quantum single-quantum (DQ-SQ) MAS NMR correlation spectrum was acquired at 10 kHz spinning frequency. POST C7 recoupling sequence[15] was used to reintroduce the ^{31}P–^{31}P homonuclear dipole-dipole interaction

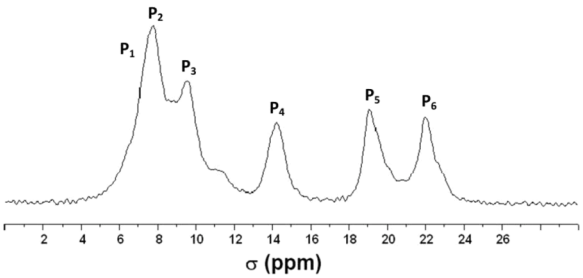

Fig. 1. ^{31}P CP-MAS spectrum of ATP(5′)Na_2•$3H_2O$ at 8 kHz showing the center band region and the identification of six phosphorus signals (P_1 – P_6).

and to achieve the excitation and reconversion of DQ coherences. The rf-field strength was ~70 kHz. Short excitation and reconversion periods of 1.5 ms were employed. 80 t_1 increments were used and 16 transients were collected each time using a recycle delay of 30 s and a presaturation sequence. For ^{23}Na 3Q experiments, a three-pulse sequence incorporating *z*-filter[16] was employed, under ^{1}H TPPM[17] decoupling during the evolution (t_1) and acquisition (t_2) periods at an rf-field of 60 kHz. The excitation (0 to ±3) and conversion (±3 to 0) steps were individually optimized and the 2D experiments were performed in the absorption mode using hyper-complex procedure [18]. Sample spinning was kept at 10 kHz and rotor synchronization during t_1 period was employed to remove spinning side bands appearing in the isotropic (δ_{iso}) dimension. Typically, 128 t_1 values were used and 360 transients were accumulated to get the desired signal to noise ratio. In all the experiments, sample spinning was regulated to within ±1 Hz using a Bruker pneumatic controller. ^{31}P and ^{23}Na spectra are externally referenced to 85% H_3PO_4 and 1 M NaCl, respectively. The ^{31} P chemical shielding tensors were determined by DMFIT [19] computer simulations of the 1D spectra extracted from 2D MAT data. The ^{23}Na quadrupolar coupling interaction parameters were first estimated from sheared 2D spectra by graphical method[20] and these were further refined by simulating and fitting the 1D MAS line shapes of each sodium site extracted from the 3Q-MAS data.

Gaussian 03 calculations

^{31}P chemical shielding and ^{23}Na EFG tensors were determined theoretically using *ab initio* quantum chemical calculations. A dimer cluster model was adapted for ATP(5′)Na_2•$3H_2O$. A molecular graphics picture of the ATP(5′)Na_2•$3H_2O$ dimer cluster is shown in Figure S3 (ESI) . The cluster contains all the six phosphorus sites and the four sodium sites for which our *ab initio* calculations are intended. The ATP (5′)Na_2•$3H_2O$ dimer cluster was built using the positional coordinates of all the atoms in the asymmetric unit [6].. Since the positions of hydrogen atoms were not determined in the X-ray structure, hydrogen atoms were added to the dimer cluster and their positions were optimized by molecular mechanics using Accelrys molecular modeling software [21]. Our calculations conform to the structure reported by Sugawara *et l* [6]. in which the correct assignment of Na4 and OW4 was made and this removes the uncertainty in the calculated results for the sodium sites. The size of the dimer cluster is large as it contains a total of 118 atoms of which 74 are heavy atoms. The crystallographic phosphorus and sodium sites of interest exist medially about the mass with minimal interactions with atoms from neighboring unit cells. This dimer is an excellent cluster model for the *ab initio* calculations of ^{31}P chemical shielding and ^{23}Na EFG tensors since it preserves the local geometry of the tri-phosphate, adenine and ribose units, the glycosidic (χ) and phosphate group (ω_1-ω_5) torsion angles, the dimer structure of sodiums (Na_1—Na_2 and Na_3—Na_4) and their coordination with phosphate oxygens and the water molecules.

The NMR shielding tensor calculations were performed using the gauge-including atomic orbital (GIAO)[22,23] method which has been used in many of the ^{31}P chemical shielding calculations on diverse molecular systems [24–27]. The calculations were carried out using Gaussian '03[28] on the dimer cluster of ATP(5′)Na_2•$3H_2O$. Initial calculations were carried out using both HF and DFT methods with increasing basis sets. HF calculations yielded faster and better convergence for the ^{31}P shieldings as the basis set was increased from STO-3G to 6–311++G(2d,2p). DFT/B3LYP calculations, on the other hand, showed good trend with experimental results at the 6–311G(2d,2p) level, although no further improvement in the computed shielding values could be made with the addition of polarization and diffuse functions whereas the B3LYP/6–311++*G*(2d,2p) calculations failed to converge even after 512 SCF cycles. In order to further improve the quality of B3LYP calculations of ^{31}P shieldings, we resorted to the locally dense approach wherein the phosphate groups, which are of our main interest, were treated with the Dunnings augmented basis set aug-cc-pVDZ(3s,2p,1d), while the ribose was treated with 6-31G(d,p) and the rest with the Slater basis. Our choice of the aug-cc-pVDZ(3s, 2p,1d) basis set on phosphorus was also guided by its stability in our DFT calculations and its superior performance in previous computations of related biological molecules [29]. The values for the principal elements (σ_{ii}), determined from Gaussian '03 calculations, are taken as absolute shieldings in ppm. These have not been converted to relative shifts with respect to 85% H_3PO_4 owing to the difficulties in calculating the absolute shielding of H_3PO_4 accurately [30].

^{23}Na EFG tensors of ATP(5′)Na_2•$3H_2O$ were determined theoretically using the Hartree-Fock method. HF calculations were carried out on the dimer cluster of ATP(5′)Na_2•$3H_2O$ using Gaussian '03 [28]. Convergence in the calculated values of ^{23}Na quadrupole couplings, both its magnitude and sign, was established as the basis set was increased from STO-3G to 6–311++G(2d,2p) (Fig. S4 ESI). The final calculations were carried out with the [6–311++G(2d,2p)] basis set. The principal elements ($V_{ii} = eq_{ii}$), determined from Gaussian '03 calculations, denote the three components ($|V_{zz}| > |V_{yy}| > |Vxx|$) of the traceless ^{23}Na EFG tensor and are expressed in atomic units (1 au = $9.71736153 \times 10^{21}$ V m^{-2}). In order to relate these to the experimentally determined quantities, namely, the quadrupole coupling constant (C_Q) and the asymmetry parameter (η_Q), the following expressions were used:

$$C_Q[MHz] = e^2q_{zz}Q/h = -243.96xQ[barn]xV_{zz}[au] \quad (1)$$

$$\eta_Q = (V_{xx} - V_{yy})/V_{zz} \quad (2)$$

where Q is the nuclear quadrupole moment of ^{23}Na, e is the elementary charge, and h is the Planck constant (6.62607015 x 10^{-34} J.Hz^{-1}). We have used the value of 0.104 barn for Q (^{23}Na) (1 barn = 10^{-28} m^2) [31, 32].

All our Gaussian '03 calculations were performed on the Grendel supercomputer system at University of Arhus, Denmark. The final DFT calculations took about two days for ^{31}P shielding and the HF calculation about four days for ^{23}Na EFG tensors.

Results and discussion

^{31}P shielding tensors in ATP(5′)Na_2•$3h_2o$

The ^{31}P chemical shielding tensors were experimentally determined in the well crystallized nucleotide ATP(5′)Na_2•$3H_2O$ by employing the MAT technique. The separation of the anisotropic spectra along the indirect dimension, at the isotropic shift of each of the peaks, has enabled us to determine the ^{31}P shielding tensor for each phosphorus site. It may be noted that this approach is superior to the determination of ^{31}P shieldings by slow-speed MAS where there is a severe overlap of spinning sidebands. For the determination of ^{31}P chemical shielding tensor of each crystallographic nonequivalent phosphorus site, it is essential that the isotropic signals are identified and assigned in ^{31}P MAS spectra.

In Fig. 1 we show the expanded center band region of the ^{31}P CP-MAS spectrum of ATP(5′)Na_2•$3H_2O$ taken at a spinning speed of 8 kHz. For

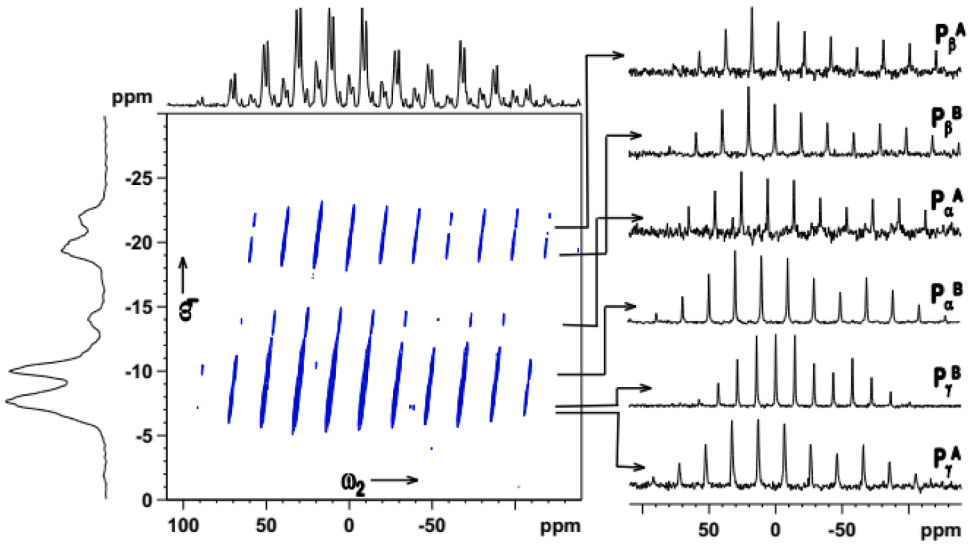

Fig. 2. ^{31}P 2D MAT contour plot of ATP(5′)Na_2•3H_2O (ν_R = 4 kHz) leading to the determination of ^{31}P shielding tensors for the six non-equivalent phosphorus sites. 1D spectra extracted parallel to ω_2 axis at the isotropic position of each of the six phosphorus sites are shown on the right.

Table 1
^{31}P chemical shielding tensors of ATP(5′)Na_2•3H_2O[a].

	σ_{11}	σ_{22}	σ_{33}	σ_{iso}	$\Delta\sigma$	η
P_γ^B	−83.9	−10.1	113.5	6.5	197.4	0.3
	(−83.9)	(−12.3)	(115.6)		(199.5)	(0.3)
P_γ^A	−81.2	−9.4	113.1	7.5	194.3	0.3
	(−75.6)	(−13.3)	(111.5)		(187.1)	(0.3)
P_α^A	−82.6	−10.7	121.8	9.5	204.0	0.3
	(−73.3)	(−11.2)	(112.9)		(186.2)	(0.3)
P_α^B	−79.6	−10.7	133.2	14.3	212.8	0.4
P_β^A	−74.1	−13.5	145.5	19.3	219.6	0.4
	(−65.7)	(−17.2)	(140.7)		(206.4)	(0.5)
P_β^B	−70.9	−9.7	146.9	22.1	17.8	0.4
	(−39.0)	(−39.0)	(144.3)		(183.3)	(1.0)

[a] From 'best fit' simulations of the anisotropic spectra (Fig. S6 ESI). Values in parentheses denote those determined from 'best fit' simulations of slow MA S spectra (Fig. S7 ESI). δ and η are given in the Herzfeld-Berger convention [34].

Table 2
Theoretically determined ^{31}P shielding tensors of ATP(5′)Na_2•3H_2O[a].

	σ_{11}	σ_{22}	σ_{33}	σ_{iso}
$\mathbf{P_\gamma^B}$	260.4	370.9	422.8	351.4
	295.1	323.5	541.1	386.5
$\mathbf{P_\gamma^A}$	250.7	392.1	430.4	357.7
	290.4	361.9	499.8	384.0
$\mathbf{P_\alpha^A}$	256.8	327.9	505.0	363.2
	297.9	352.3	517.1	389.1
$\mathbf{P_\alpha^B}$	266.1	330.4	521.1	372.5
	306.6	347.2	534.4	396.1
$\mathbf{P_\beta^A}$	302.3	353.7	470.4	375.5
	336.3	377.4	503.1	405.6
$\mathbf{P_\beta^B}$	292.3	348.6	482.6	374.5
	311.3	351.7	543.6	402.2

[a] Values are given as absolute shieldings in ppm, determined from Gaussian '03 HF/6–311++*G*(2d,2p) (first row) and B3LYP/(aug-cc-pDVZ(3 s,2p,1d),6–31G(d,p) (second row) calculations.

the six crystallographic non-equivalent phosphorus sites in ATP(5′)Na_2•3H_2O dimer, the ^{31}P CP-MAS spectrum reveals five peaks which are well resolved, with the peak corresponding to the sixth site appearing as a shoulder at the low-field end of the spectrum. The observed ^{31}P CP-MAS spectrum is identical to that observed previously at 90% relative humidity which was shown to correspond to the trihydrate [6,8]. Our Na_2ATP sample indeed conforms to the trihydrate form and has very

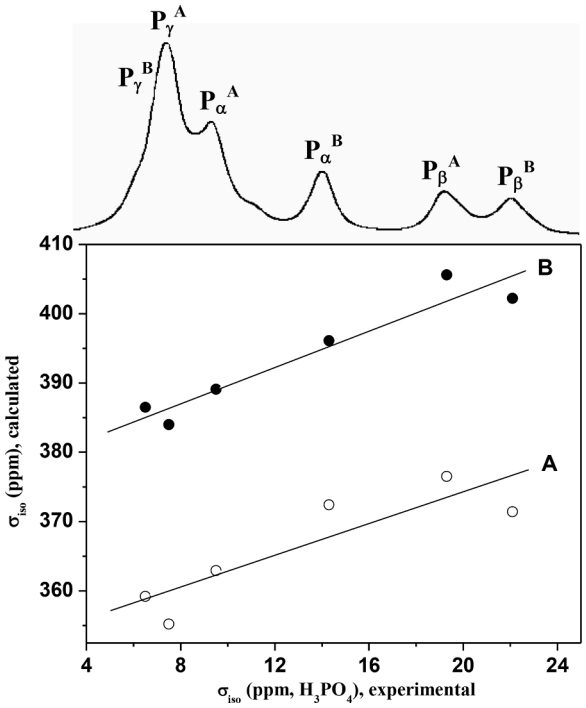

Fig. 3. Comparison of the experimental ^{31}P isotropic chemical shifts (Table 1) with the theoretically calculated isotropic shieldings (Table 2) of ATP(5′)Na_2•3H_2O. (o) HF/6–311++*G*(2d,2p); (•) B3LYP/(aug-cc-pDVZ(3 s,2p,1d),6–31G(d,p)). The signal assignment based on the POST-C7 experiment and *ab initio* calculation is shown in the ^{31}P MAS spectrum above. The straight lines represent a linear least-squares fit to the data.

little contamination from 2H_2O. For the sake of convenience, the six signals are labeled as P_1 to P_6 and these occur at 6.5, 7.5, 9.5, 14.3, 19.3, and 22.1 ppm (in the σ scale) from 85% H_3PO_4. However, the assignment of each of these resonances to correct crystallographic sites in molecules A and B of the dimer is not known *a priori*. Since our main interest is to determine ^{31}P shielding tensors for all the six phosphorus sites in the dimer structure, the assignments of the resonances P_1-P_6 to the correct crystallographic sites must be made first.

In order to aid the ^{31}P signal assignments we employed the two

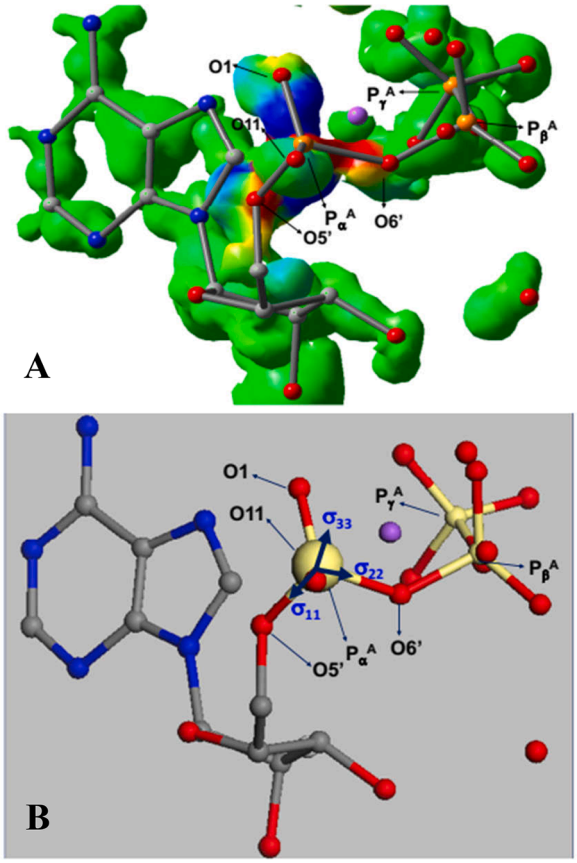

Fig. 4. (**A**) Shielding density seen by P_α^A in the ZZ direction mapped between in the range −1.214 – 1.214 on the Current Density = Z isosurface at a value of 0.003. Red corresponds to the value of –1.214 (deshielding) and blue to the value of +1.214 (shielding). The molecular skeleton corresponding to the shielding density surface is shown as an overlay. Hydrogen atoms included in the calculation and which contribute to the current density surface are not shown for clarity. (**B**) The orientation of the ^{31}P chemical shielding tensor of P_α^A with the most shielded direction nearly perpendicular to the plane defined by the phosphorus and the two bridging oxygens O5′ and O6′. The free atoms correspond to sodium (purple) and water oxygen (red) respectively. ^{31}P shielding tensor orientations of all the six phosphorus sites are depicted in Fig. S9 (ESI).

dimensional ^{31}P POST-C7 experiment[15]. The symmetry-based POST C7 sequence mediates recoupling of the dipolar interaction between ^{31}P spins under MAS and provides information about triphosphate P-P connectivity in the structure. The dipolar correlation of DQ (ω_1) and SQ (ω_2) frequencies for the direct and distant P-P dipolar interactions in the ATP(5′)Na_2•$3H_2O$ dimer is shown in Fig. S5 (ESI). Pair-wise DQ-SQ correlations are established for each of the four pairs of dipole-dipole interactions, two from each monomer. The strong cross-peaks in the 10 to 30 ppm range in the DQ dimension originates from the intermolecular P^γ-P^γ dipolar interaction between the two monomers at a distance of 4.15 Å which is comparable to the end-to-end intramolecular distances 4.27 Å and 4.53 Å for the two P^α-P^γ interactions. With the above observations and by assigning the ^{31}P resonance at the extreme high-field end of the spectrum to P^β of one monomer [33], the corresponding P^α and P^γ assignments in the same monomer can be made. The assignment of α, β, and γ sites is found to be in conformity with the solution state ^{31}P spectra[24,33] for the ATP monomer. Similarly, the phosphorus sites in the other monomer can be identified and assigned from the 2D spectrum (α', β', γ'). However, the exact assignment of these resonances to the A and B molecules in the structure cannot be made from the 2D POST-C7 experiment. The assignment of the signals to the A and B molecules of the dimer could be made on the basis of *ab initio* calculations of ^{31}P chemical shielding tensors (*vide infra*).

Table 3
Orientation of ^{31}P shielding tensors of ATP(5′)Na_2•$3H_2O$ determined from B3LYP/AUG-cc-pDVZ(3 s,2p,1d) calculations.

Phosphorus site	Tensor element	Angle between σ_{ii} and P-O Bond[a]			
P_α^A	σ_{11}	60.0 (O5)	158.3 (O6')	76.5 (O1)	83.5 (O11)
	σ_{22}	30.4 (O5')	69.9 (O6')	127.8 (O1)	109.0 (O11)
	σ_{33}	85.6 (O5')	82.2 (O6')	41.0 (O1)	159.9 (O11)
P_β^A	σ_{11}	138.6 (O7')	40 (O6')	89.2 (O2)	91.2 (O22)
	σ_{22}	49.1 (O7')	51 (O6')	113.7 (O2)	126.4 (O22)
	σ_{33}	84.6 (O7')	82.8 (O6')	156.2 (O2)	36.5 (O22)
P_γ^A	σ_{11}	156.8 (O7')	51.8 (O3)	85.9 (O33)	89.2 (O333)
	σ_{22}	112.7 (O7')	141.8 (O3)	58.8 (O33)	52.3 (O333)
	σ_{33}	94.3 (O7')	91.9 (O3)	148.5 (O33)	37.7 (O333)
P_α^B	σ_{11}	132 (O5)	28.7 (O6')	25 (O1)	146.8 (O11)
	σ_{22}	42.7 (O5)	61.5 (O6')	114.7 (O1)	122.9 (O11)
	σ_{33}	96.1 (O5)	87.4 (O6')	25 (O1)	146.8 (O11)
P_β^B	σ_{11}	140.7 (O7')	38.9 (O6')	92.4 (O2)	90.9 (O22)
	σ_{22}	129.3 (O7')	128.9 (O6')	64 (O2)	52 (O22)
	σ_{33}	89 (O7')	90.2 (O6')	153.9 (O2)	38 (O22)
P_γ^B	σ_{11}	40.5 (O7')	139.2 (O3)	87 (O33)	90.3 (O333)
	σ_{22}	49.6 (O7')	50 (O3)	128.6 (O33)	112.3 (O333)
	σ_{33}	88.2 (O7')	83.5 (O3)	38.7 (O33)	157.7 (O333)

[a] In degrees. The oxygen atom involved in the P-O bond is given in parenthesis and the numbering is as in the X-ray structure by Sugawara *et al* [6].

Two dimensional MAT experiment was used for the determination of ^{31}P chemical shielding tensors of the six phosphorus sites in ATP(5′)Na_2•$3H_2O$ dimer Fig. 2. shows the contour plot of 2D MAT data. From the observed correlation of anisotropic chemical shielding with the corresponding isotropic shift, we were able to extract the anisotropic line shapes for each of the six phosphorus sites in the structure. Spinning sidebands appear in the anisotropic spectrum along the ω_2 dimension as the MAT experiment was conducted at 4 kHz spinning speed. The anisotropic spectra of the six phosphorus sites, extracted from the 2D MAT data matrix at the isotropic peak positions, are shown alongside in Fig. 2. The anisotropy parameters (Δσ, η)[34] determined from computer simulations of these spectra (Fig. S6: ESI) yielded the principal elements of the ^{31}P chemical shielding tensor for each of the six phosphorus sites and these are given in Table 1. ^{31}P chemical shielding parameters were also determined from variable speed MAS spectra recorded at 4, 6, and 8 kHz spinning speeds and subjecting them to computer simulations. (Fig. S7: ESI) Although the shielding parameters determined from slow MAS analysis compared quite well with MAT results, the ^{31}P shielding tensors determined from MAT experiments were considered to be more accurate for comparison with the theoretically determined ^{31}P shielding tensors.

Calculations of ^{31}P shielding tensors

The ^{31}P shielding tensors resulting from the final HF and DFT Gaussian '03 calculations are given in Table 2. Based on the P-P dipolar connectivity established in the POST-C7 experiment (*vide supra*), the six

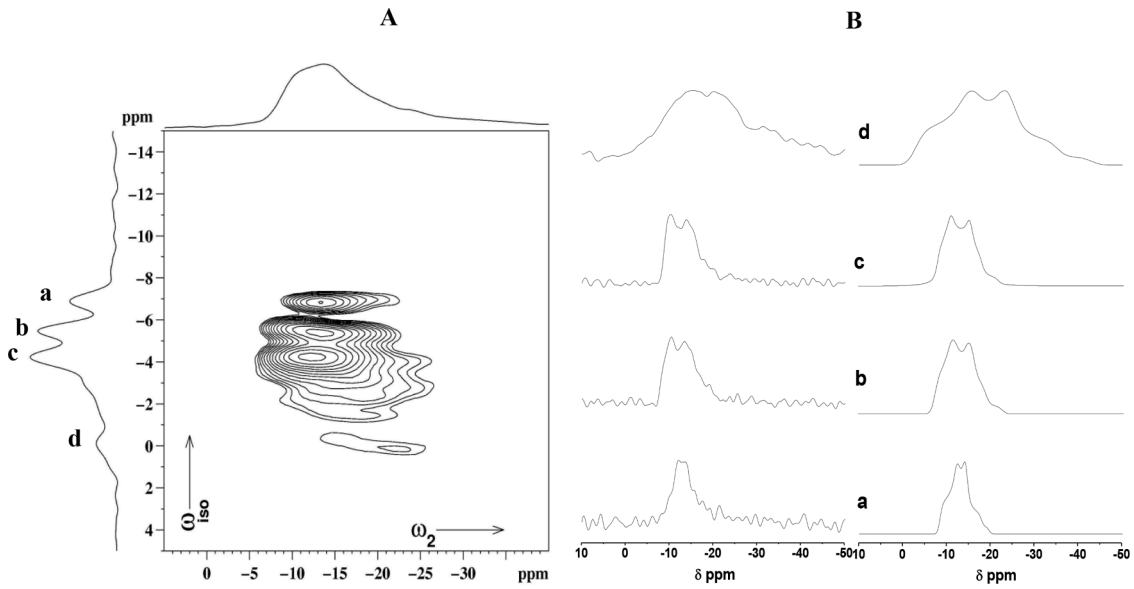

Fig. 5. (**A**) Sheared ^{23}Na (^{1}H decoupled) 3Q-MAS spectrum of ATP(5′)Na_2•$3H_2O$ showing the resolution of the four sodium sites. (**B**) 1D MAS spectra for the four sodium sites extracted from the 3Q-MAS spectrum (left) and the 'best fit' simulated spectra (right).

Table 4
^{23}Na quadrupole and chemical shift parameters ATP(5′)Na_2•$3H_2O$ from 3Q-MAS[a].

Signal	Na assignment	C_Q (MHz)	η_Q	δ_{CS} (ppm)	δ_{iso}(ppm)	P_Q
a	Na1/Na2	1.05 (1.1)	0.66 (0.7)	−8.06	(0.0)	1.123 (1.186)
b	Na1/Na2	1.25 (2.1)	0.45 (0.5)	−6.6	(0.5)	1.292 (2.186)
c	Na4	1.21 (1.6)	0.37 (0.9)	−7.0	(1.6)	1.237 (1.803)
d	Na3	1.95 (2.3)	0.54 (0.5)	−2.55	(−1.9)	2.043 (2.394)

[a] δ_{iso}denotes isotropic shift and δ_{CS} the chemical shift. $P_Q = C_Q(1+\eta^2/3)^{1/2}$. Values in parentheses denote the values reported by Grant et al [10]. The sodium site assignments based on HF/6–311++G(2d,2p) calculations are indicated.

Table 5
^{23}Na EFG tensors of ATP(5′)Na_2•$3H_2O$ from HF/6–311++G(2d,2p) calculations[a].

Na site	Eigen Values			C_Q[b]	η_Q	P_Q
	V_{xx}	V_{yy}	V_{zz}			
Na_1	−0.046538	−0.096943	0.143482	−3.506	0.351	−1.644
Na_2	0.001040	0.115814	−0.116853	2.855	0.982	2.008
Na_3	−0.007009	−0.130109	0.137119	−3.351	0.898	2.371
Na_4	−0.030089	−0.092850	0.122940	−3.004	0.511	−1.421

[a] EFG tensor elements are calculated in atomic units (au) by Gaussian'03. C_Q was calculated using Eq. (1) with a value of 0.104 barn for the quadrupole moment (eQ) of ^{23}Na.

resonances in the ^{31}P CP-MAS spectrum could be identified and ascribed in a pair wise manner to the P_α, P_β, and P_γ sites in the two ATP molecules in the asymmetric unit. However, the exact assignment of the ^{31}P signals to the six crystallographic nonequivalent sites in the structure could not be made from the experimental data alone since *α, β, γ* sites of A and B one molecule (A) are not distinguished from the other (B). This distinction can, however, be made from our quantum chemical calculations. When we examine the correspondence between the experimental shieldings and the theoretically calculated isotropic shieldings

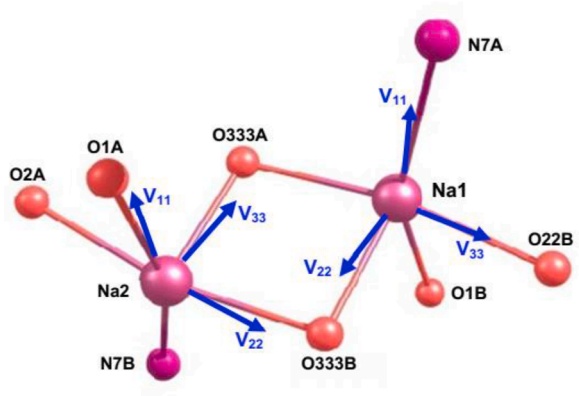

Fig. 6. The orientation of the ^{23}Na EFG tensor of tightly bound Na1 and Na2 sites in the sodium centered Cartesian frame. The sodium coordination with the bridging oxygens, the phosphate oxygens and the base nitrogens of the ATP dimer is shown and with the atom numbers conforming to the X-ray structure of Sugawara et al. [6].

for the two possible assignments, only one gives good correlation. This is shown in Fig. 3 for both the HF/6–311++G(2d,2p) (**A**) (R = 0.877, rmsd = 1.51 ppm) and the B3LYP/(aug-cc-pDVZ(3s,2p,1d), 6–31G(d,p)) (**B**) (R = 0.956, rmsd = 0.96 ppm) calculations. As seen, our B3LYP/(aug-cc-pDVZ(3s,2p,1d), 6–31G(d,p)) results show superior correlation to the experimental data. Among the three chemically distinct phosphorus environments, P_α shows the largest dispersion in the experimental chemical shift for the A and B molecules (4 ppm), while this is smaller for P_β (2 ppm) and P_γ (1 ppm). These are in good agreement with the B3LYP/(aug-cc-pDVZ(3s,2p,1d), 6–31G(d,p)) values of 7, 2.5, and 1.4 ppm for P_α, P_β and $P_{\gamma'}$ respectively, for the assignment shown in Fig. 3. Thus, based on *ab initio* ^{31}P chemical shielding calculations, all the resonances can be assigned with confidence for the first time in the ^{31}P CP-MAS spectrum.

From our *ab initio* calculations, we gather additional insights on the bearing that the local conformation has on ^{31}P chemical shieldings. We mainly focus on the P_α site for which the shift between the two conformers (A and B) is the largest (4 ppm). It is recognized that the chemical shift of the P_α site is influenced by the two sets of R-O-P-O (R')

Table 6
Orientation of ^{23}Na electric field gradient tensors of ATP(5′)Na_2•3H_2O determined from HF/6–311++*G*(2d,2p) Calculations.

Na site	Tensor element	Angle between V_{ii} and N—O Vector[a]					
Na1		Na1-O333A	Na1-O1B	Na1-O22B	Na1-O333B	Na1-N7A	Na-Na2
	V11	94.39	161.27	81.99	93.27	14.03	93.64
	V22	79.04	93.19	85.45	5.75	103.87	37.30
	V33	168.17	71.56	9.23	85.29	92.1	127.06
Na2		Na2-O1A	Na3-O2A	Na2O333A	Na2-O333B	Na2-N7B	Na2-Na1
	V11	13.01 (O1)	91.62 (O5)	95.54 (O9)	87.63 (O22)	166.66(N8)	90.64
	V22	102.59	178.37	99.00	12.60	91.95	56.29
	V33	86.79	90.18	10.59	77.63	103.20	33.72
Na3		Na3-O2A	Na3-OW1	Na3-OW3	Na3-OW61	Na3-Na4	
	V11	80.70	118.72	41.63	132.64	88.94	
	V22	104.92	90.40	124.93	136.94	34.97	
	V33	16.31	28.72	70.32	94.97	124.95	
Na4		Na4-O11A	Na4-OW2	Na4-OW61	Na4-Na3		
	V11	59.86	32.91	130.25	63.96		
	V22	95.45	94.12	108.54	145.67		
	V33	149.27	57.41	46.06	69.27		

[a] In degrees. The oxygen atom involved in the coordination with each sodium is indicated above each entry. The atom numbering is as per the X-ray structure of Sugawara *et al* [6].

torsion angles ω_1 and ω_2, with a gauche (g)-gauche (g) configuration causing more shielding compared to the gauche (g)-trans (t) configuration [35,36]. From the crystal structure data[6] of ATP(5′)Na_2•3H_2O, these values are found to be: $\omega_1 = 72^\circ$ (A), -45° (B) and $\omega_2 = 152^\circ$ (A), -76° (B). Thus, we can infer that the local conformation for P_α in the A molecule is gauche-gauche while that in the B molecule is gauche-trans. This implies an upfield shift for the P_α^A resonance over P_α^B, in excellent agreement with the experimental results and theoretical calculations, further lending credence to our assignment.

The eigen values of the principal components σ_{ii} of the ^{31}P shielding tensor determined from B3LYP/(aug-cc-pDVZ(3s,2p,1d),6–31G(d,p)) calculations are compared with those determined experimentally by 2D MAT in Fig. S8 (ESI). The three shielding components are well demarcated for the six phosphorus sites. σ_{11} and σ_{22} elements are closer (28–72 ppm) as compared to σ_{22} and σ_{33} (126–218 ppm). The total range covered between the shielding and deshielding extremes is 167–246 ppm and is comparable to the 194–220 ppm determined from MAT experiments. It is also seen that none of the shielding tensors is completely axially symmetric. For all the phosphorus sites the skew value is positive. This is due to the fact that in each case the intermediate shielding occurs close to the deshielding extreme. It can also be seen that for many of the sites the tensor is far from non-axial symmetry. A similar feature can also be noticed in the experimentally determined ^{31}P tensors. Although a one to one correspondence cannot be established for a given site from the calculated shielding values of all the principal components, presumably due to the observed dispersion in each set of principal values, the isotropic values do show a very good correlation with experiment as established in Fig. 3.

We present in Fig. 4, the orientation of the ^{31}P chemical shielding tensor determined for P_α^A from the *ab initio* calculations. The orientation of the three principcal elements in the molecule fixed Cartesian frame and the shielding density determined at this phosphorus site are depicted in Fig. 4. ^{31}P shielding tensor orientations of all the six phosphorus sites were determined with the aid of EFGSHIELD[32] program. In each case the triphosphate moiety is shown, with labels only on the four bonded oxygens (Fig. S9: ESI) Table 3. gives the angle between the principal elements (σ_{ii}) and the immediate four P-O bonds.

The data presented in Table 3 show how the principal elements of the shielding tensor on each phosphorus center are oriented with respect to the P-O bond vectors. A striking observation that comes out from this data about the orientation of ^{31}P shielding tensors is that for all the six phosphorus sites the most shielded direction is nearly perpendicular to the plane defined by the phosphorus center and two adjoining oxygens as visualized for P_α^A in Fig. 3B. The maximum deviation from this orientation is no larger than 7° noticed only in two of the six phosphorus sites. For P_α and P_β, both in A and B molecules, the oxygens involved are the two bridging ones (P-O-P), whereas for the P_γ sites the bridging and a terminal oxygen are involved. Our results are in general agreement with the tensor orientations given in a previous study [11], where these were mainly determined for knowing the orientation of various P-P dipolar vectors with respect to the chemical shielding tensor, required for the simulation of ^{31}P-^{31}P double quantum buildup curves. It may be pointed out that the previously reported results of *ab initio* calculations had been carried out at a lower computational and basis level, namely B3PW91/6–31G, while our calculations are based on a better DFT functional (B3LYP) using optimally chosen basis sets [37]. Furthermore, it is not clear whether the previous calculations[11] were based on the well determined X-ray structure data of Sugawara *et al*.[6] We therefore believe that the principal values and eigen vectors of ^{31}P chemical shielding tensors have been more determined in the present study with increased numerical accuracy.

^{23}Na electric field gradients in ATP(5′)Na_2•3h_2o

The dimer structure of ATP(5′)Na_2•3H_2O presents four nonequivalent sodium environments and these cannot be distinguished in conventional magic angle spinning experiments due to severe second-order quadrupolar broadening (Figure S10 ESI). However, the four crystallographic nonequivalent sodium sites in the structure are identified by the dipolar decoupled z-filter triple-quantum magic-angle-spinning experiment[16]. The sheared 3Q-MAS spectrum of ATP(5′)Na_2•3H_2O is shown in Fig. 5. The observed Na site resolution was facilitated by enhanced second-order quadrupolar effects at 7.01 T and the application of ^{1}H decoupling using TPPM[17] during 3Q evolution and 1Q observation periods [38]. The four nonequivalent sodium sites in the structure of ATP(5′)Na_2•3H_2O, resolved in the isotropic spectrum, are marked as (**a**-**d**) in the figure. The expected sodium site occupancy is not readily apparent due to unequal 3Q excitation efficiencies[39] for all the Na sites. Nevertheless, for the four crystallographic nonequivalent sodium sites in the dimer structure of ATP(5′)Na_2•3H_2O, the 3Q-MAS spectrum of Fig. 5 provides valuable data on the chemical shielding and electric field gradient parameters and aid the structural assignment. ^{23}Na isotropic chemical shielding (δ_{CS}) and the quadrupolar interaction parameter [$P_Q = C_Q(1+\eta^2/3)$] were first determined by a graphical analysis[20] of the 3Q-MAS contour data plotted in the universal δ_2 and δ_{iso}ppm scales [20,40]. ^{23}Na electric field gradients, characterized by the quadrupole coupling constant ($C_Q = eQV_{ZZ}/h = e^2qQ/h$) and the asymmetry parameter $\eta_Q = (V_{XX}\text{-}V_{YY})/V_{ZZ}$, where V_{XX}, V_{YY}, and V_{ZZ} are the principal elements of the traceless EFG tensor, were finally determined from computer simulations of MAS spectra corresponding to each Na site. The experimental and simulated ^{23}Na MAS spectra are shown in

Fig. 5 and the 'best fit' values of the chemical shift and EFG parameters for the four sodium sites are given in Table 4.

In the well crystallized sample with no admixture of dehydrate present, the four resonances (**a–d**) (Fig. 5) correspond to the four nonequivalent sodium sites in the ATP(5′)Na_2•$3H_2O$ structure determined by Sugawara *et al.* [6]. Of the four isotropic peaks (**a-d**) resolved by 3Q-MAS, the resonances **c** and **d** are assigned to the sodium sites Na4 and Na3, respectively, in the structure. This assignment follows the previous study of ATP(5′)Na_2•$3H_2O$ by Grant et al.[10] who employed ^{23}Na-^{31}P MQ-REDOR and site resolved ^{23}Na T_1 experiments for the signal assignment. The guiding factor to making this assignment in our study is the resolution of the four distinct sodium sites in 3Q-MAS, in the same manner as in the previous study [10], and a comparable dispersion in the values of P_Q and δ_{CS} for the peaks **c** and **d** in the 3Q-MAS spectrum and in the theoretically calculated values of the quadrupolar couplings (*vide infra*). However, as in the previous study [10], the signals **a** and **b** are marked by a small difference in their P_Q (0.17 MHz) and δ_{CS} (1.5 ppm) values and hence could not be assigned to the two other Na sites in the structure on the basis of experimental results alone.

HF calculations of ^{23}Na EFG tensors

^{23}Na EFG tensors determined from HF/6–311++G(2d,2p) calculations are given in Table 5 along with the C_Q and η_Q values estimated from the tensor components using Eqs. 1, (2). ^{23}Na EFGs have been determined with a high numerical accuracy at the highest basis level [6–311++G(2d,2p)]. Further, previously reported[9,41] *ab initio* calculations of ^{23}Na EFGs in ATP(5′)Na_2•$3H_2O$ were based on the ATP model derived from the original X-ray structure [5]. In view of the interchanged assignment of Na_4 and OW_4 atoms in the work of Sugawara *et al.* [6]., the previously reported calculations are likely to suffer from uncertainties in the calculated quadrupole couplings. This is corrected in our work and, besides, we have determined the ^{23}Na electric field gradient tensors with a high numerical accuracy at the highest basis level [6–311++G(2d,2p)] which was not done before.

As seen from the results of Table 5, the four sodium sites are demarcated by their absolute quadrupole couplings spanning the range 2.9–3.5 MHz, in comparison with the 1.1 – 2.0 MHz span seen in the experimental results (Table 4). Since the calculations are carried out for a rigid structure, the reduction seen in the experimental values of quadrupole couplings is likely due to motional effects. For the sodium sites already assigned, namely, Na3 and Na4, the absolute values of C_Q determined from HF/6–311++*G*(2d,2p) calculations are 3.4 and 3.0 MHz, respectively. The observed decrease seen from the 3Q-MAS values of 2.0 and 1.2 MHz for the peaks **c** and **d**, respectively, is in accord with those reported by Grant *et al.* [10]. For the other two sodium sites, namely Na1 and Na2, the calculations yield absolute quadrupole coupling constants of 2.9 and 3.5 MHz, respectively, whereas the experimentally determined C_Q values mark a much smaller difference (0.2 MHz) for the **a** (1.1 MHz) and **b** (1.3 MHz) sites and preclude their assignment in 3Q-MAS. ^{23}Na MQ-MAS experiments at very low temperature would be helpful in this regard but this could not be pursued in the present study. The ^{23}Na EFG parameters along with the associated values for the second-order quadrupole shift parameter [$P_Q = C_Q(1+\eta^2/3)^{1/2}$] are given in Table 4. It may be noted that our *ab inito* calculations also yield the sign of the quadrupole coupling which cannot be determined from our NMR experiments [42].

Our ^{23}Na *ab initio* calculations also yield the eigenvectors for the principal elements of the ^{23}Na EFG tensor expressed in the Na centered Cartesian frame. These in turn are used to derive the orientation of the three principal elements with respect to the Na-O coordination bond for the four Na sites in the ATP(5′)Na_2•$3H_2O$ structure. These were obtained using the EFGSHIELD[32] program. The X-ray structure report of Sugawara *et al.* [6]. indicates that of the four inequivalent sodium sites, Na1 and Na2 are tightly bound to the triphosphate chains whereas the other two sites Na3 and Na4 are coordinated by the anionic oxygens of the phosphates and water molecules with Na4 existing in a labile coordination environment. For the tightly bound Na1 and Na2 the electric field gradient tensor orientation determined from our HF/level 6–311++*G*(2d,2p) calculations is shown in Fig. 6. This depicts how the three principal elements of the electric field gradient tensor are oriented with respect to the coordination bonds between Na1 and Na2 and the bridging oxygens, the phosphate oxygens and the base nitrogens of the ATP dimer Table 6gives the angle between the principal elements (Vii) and the Na-O bond vectors.

The data presented in Table 6 show that for the tightly bound Na1 and Na2 sites the smallest EFG felt by these sites is along the direction which is nearly perpendicular to the plane defined by the sodium center and the coordinating oxygens (O22B, O333B) and (O333A, O333B). Our results further show that the electric field gradient is the largest along the direction leading to O333A and O22B for the sites Na1 and Na2, respectively, whereas intermediate field gradient felt by these sites lies closer to the direction leading to one of the bridging oxygens, namely O333B. No such characteristic feature of the tensor orientation with respect to their local coordination can be readily discerned from the orientation angles determined for the for the Na3 and Na4 sites.

Conclusions

In conclusion, the combination of solid-state ^{31}P and ^{23}Na MAS NMR spectroscopy and *ab initio* quantum chemical calculations is an effective strategy to provide structural characterization in terms of their associated ^{31}P chemical shielding and ^{23}Na EFG tensors. The experimental assessment of the ^{31}P-^{31}P dipolar connectivity within and between the two triphosphate chains of the ATP dimer and the determination of ^{31}P shielding tensors by B3LYP/(aug-cc-pDVZ(3s,2p,1d), 6–31G(d,p)) quantum chemical calculations have enabled a structure-based resonance assignment to be made in ^{31}P CP-MAS spectra. The difference in triphosphate conformation of the A and B molecules of the ATP dimer and the altered geometry at the $^{31}P_{\alpha,\beta,\gamma}$ sites largely determine the eigen values of the observed ^{31}P shielding tensors with no major perturbations to their orientation in a molecule fixed frame. This suggests that ^{31}P tensors would be strongly coupled to the crystal transition between the di- and tri-hydrate forms ensuing from the conformational changes induced in the crystal transition. The HF/6–311++G(2d,2p) calculations of ^{23}Na electric field gradients have enabled a structural characterization of the four sodium sites in the ATP(5′)Na_2•$3H_2O$ dimer structure, besides aiding a partial resonance assignment of the ^{23}Na 3Q-MAS spectrum. For the two sodium sites which are tightly coordinated the orientation of the EFG tensor is distinctive with unique directions along which the field gradient is the smallest and largest.

Declaration of Competing Interest

The authors declare that they have no known competing financial interests or personal relationships that could have appeared to influence the work reported in this paper. The authors declare the following financial interests/personal relationships which may be considered as potential competing interests: P. K. Madhu

Acknowledgements

S.G. thanks the Council of Scientific and Industrial Research, New Delhi, India for support under Emeritus Scientist Scheme (HRDG:21 (0701)/ 07/EMR-II). G.S thanks Dr. Krishnan Damodaran for discussions on *ab initio* calculations. PKM acknowledges intramural funds at TIFR Hyderabad from the Department of Atomic Energy (DAE), India, under Project Identification Number RTI 4007. We dedicate this article to Shimon Vega, who unfortunately passed away on November 16, 2021.

Supplementary materials

Supplementary material associated with this article can be found, in

the online version, at doi:10.1016/j.jmro.2022.100051.

References

[1] K Lohmann, Über die pyrophosphatfraktion im muskel, Naturwissenschaften 17 (1929) 624–625, https://doi.org/10.1007/BF01506215.

[2] J. Baddiley, A.M. Michelson, A.R. Todd, Nucleotides. Part II. A synthesis of adenosine triphosphate, J. Chem. Soc. (1949) 582–586, https://doi.org/10.1039/JR9490000582.

[3] L. Grycova, P. Sklenovsky, Z. Lansky, M. Janovska, M. Otyepka, E. Amler, J. Teisinger, M. Kubala, ATP and magnesium drive conformational changes of the Na+/K+-ATPase cytoplasmic headpiece Biochim, Biophys. Act. (BBA). 1788 (2009) 1081–1091, https://doi.org/10.1016/j.bbamem.2009.02.004.

[4] O. Kennard, N.W. Isaacs, W.D.S. Motherwell, J.C. Coppola, D.L. Wampler, A. C. Larson, D.C. Watson, The crystal and molecular structure of adenosine triphosphate, Proc. Royal Soc. London. Ser. A. 325 (1971) 401–436, https://doi.org/10.1098/rspa.1971.0177.

[5] A.C. Larson, Restrained refinement of disodium adenosine 5′-triphosphate trihydrate, Acta Crystallogr B34 (1978) 3601–3604, https://doi.org/10.1107/S0567740878011693.

[6] Y. Sugawara, N. Kamiya, H. Iwasaki, T. Ito, Y. Satow, Humidity-controlled reversible structure transition of disodium adenosine 5′-triphosphate between dihydrate and trihydrate in a single crystal state, J. Am. Chem. Soc. 113 (1991) 5440–5445, https://doi.org/10.1021/ja00014a041.

[7] H. Urabe, Y. Sugawara, T. Kasuya, Humidity-dependent structural transition of guanosine and disodium adenosine 5'-triphosphate crystals studied by low-frequency Raman spectroscopy, Phys. Rev. 51 (1994) 5666–5672, https://doi.org/10.1103/PhysRevB.51.5666.

[8] Y. Shindo, A. Naito, S. Tuzi, Y. Sugawara, H. Urabe, H. Saito, Stepwise conformational transition of crystalline disodium adenosine 5′-triphosphate with relative humidity as studied by high resolution solid state 13C and 31P NMR, J. Mol. Struct. 602-603 (2002) 389–397, https://doi.org/10.1016/S0022-2860(01)007219.

[9] A. Wong, G. Wu, Characterization of the Pentacoordinate Sodium Cations in Hydrated Nucleoside 5 '-Phosphates by Solid-State 23Na NMR and Quantum Mechanical Calculations, J. Phys. Chem. A. 107 (2003) 579–586, https://doi.org/10.1021/jp021937k.

[10] C.V. Grant, D. McElheny, V. Frydman, L. Frydman, Solid-state NMR investigation of sodium nucleotide complexes, Magn. Reson. Chem. 44 (2006) 366–374, https://doi.org/10.1002/mrc.1750.

[11] M.J. Potrzebowski, J. Gajda, W. Ciesielski, I.M. Montesinos, Distance measurements in disodium ATP hydrates by means of 31P double quantum two-dimensional solid-state NMR spectroscopy, J. Magn. Reson. 179 (2006) 173–181, https://doi.org/10.1016/j.jmr.2005.11.016.

[12] Z. Gan, High-resolution chemical shift and chemical shift anisotropy correlation in solids using slow magic angle spinning, J. Am. Chem. Soc. 114 (1992) 8307–8309, https://doi.org/10.1021/ja00047a062.

[13] L. Frydman, J.S. Harwood, Isotropic spectra of half-integer quadrupolar spins from bidimensional magic-angle spinning NMR, J. Am. Chem. Soc. 117 (1995) 5367–5368, https://doi.org/10.1021/ja00124a023.

[14] J.Z. Hu, W. Wang, F. Liu, M.S. Solum, D.W. Alderman, R.J. Pugmire, D.M. Grant, Magic-angle-turning experiments for measuring chemical-shift-tensor principal values in powdered solids, J. Magn. Reson. Ser. A. 113 (1995) 210–222, https://doi.org/10.1006/jmra.1995.1082.

[15] M. Hohwy, H.J. Jakobsen, M. Edén, M.H. Levitt, N.C. Nielsen, Broadband dipolar recoupling in the nuclear magnetic resonance of rotating solids: A compensated C7 pulse sequence, J. Chem. Phys. 108 (1998) 2686–2694, https://doi.org/10.1063/1.475661.

[16] J.P. Amoureux, C. Fernandez, S. Steuernagel, Z-Filtering in MQMAS NMR, J. Magn. Reson. 123 (1996) 116–118, https://doi.org/10.1006/jmra.1996.0221.

[17] A.E. Bennett, C.M. Rienstra, M. Auger, K.V. Lakshmi, R.G. Griffin, Heteronuclear decoupling in rotating solids, J. Chem. Phys. 103 (1995) 6951–6958, https://doi.org/10.1063/1.470372.

[18] D. States, R. Haberkorn, D. Ruben, A two-dimensional nuclear Overhauser experiment with pure absorption phase in four quadrants, J. Magn. Reson. 48 (1982) 286–292, https://doi.org/10.1016/0022-2364(82)90279-7.

[19] D. Massiot, F. Fayon, M. Capron, I. King, S. Le Calvé, B. Alonso, J –O Durand, B. Bujoli, Z. Gan, G. Hoatson, Modelling one-and two-dimensional solid-state NMR spectra, Magn. Reson. Chem. 40 (2002) 70–76, https://doi.org/10.1002/mrc.984. This program is available at: http://crhmt-europe.cnrs orleans.fr/dmfit/help/dmfit.htm.

[20] J.P. Amoureux, C. Fernandez, Triple, quintuple and higher order multiple quantum MAS NMR of quadrupolar nuclei, Solid State NMR 10 (1998) 211–223, https://doi.org/10.1016/S0926-2040(97)00027-1.

[21] Materials Studio, Accelrys Software Inc, 2001. Accelrys. ©-2007.

[22] R. Ditchfield, Self-consistent perturbation theory of diamagnetism: I. A gauge-invariant LCAO method for NMR chemical shifts, Mol. Phys. 27 (1974) 789–807, https://doi.org/10.1080/00268977400100711.

[23] K. Wolinski, J.F. Hinton, P. Pulay, Efficient implementation of the gauge-independent atomic orbital method for NMR chemical shift calculations, J. Am. Chem. Soc. 112 (1990) 8251–8260, https://doi.org/10.1021/ja00179a005.

[24] D.G. Gorenstein, D.O. Shah, Phosphorus-31 NMR Principles and Applications, Academic Press, Orlando, 1984. Chapter 18.

[25] Sun Un, M.P. Klein, Study of prosphorus-31 NMR chemical shift tensors and their correlation to molecular structure, J. Amer. Chem. Soc. 111 (1989) 5119–5124, https://doi.org/10.1021/ja00196a015.

[26] C. van Wullen, A comparison of density functional methods for the calculation of phosphorus-31 NMR chemical shifts, Phys. Chem. Chem. Phys. 2 (2000) 2137–2144, https://doi.org/10.1039/B000461H.

[27] T.M. Alam, Ab initio calculations of 31P NMR chemical shielding anisotropy tensors in phosphates: variations due to ring formation, Int. J. Mol. Sci. 3 (2002) 888–906, https://doi.org/10.3390/i3080888.

[28] M.J. Frisch, G.W. Trucks, H.B. Schlegel, G.E. Scuseria, M.A. Robb, J.R. Cheeseman, J.A. Montgomery Jr., T. Vreven, K.N. Kudin, J.C. Burant, J.M. Millam, S.S. Iyengar, J. Tomasi, V. Barone, B. Mennucci, M. Cossi, G. Scalmani, N. Rega, G.A. Petersson, H. Nakatsuji, M. Hada, M. Ehara, K. Toyota, R. Fukuda, J. Hasegawa, M. Ishida, T. Nakajima, Y. Honda, O. Kitao, H. Nakai, M. Klene, X. Li, J.E. Knox, H. P. Hratchian, J.B. Cross, V. Bakken, C. Adamo, J. Jaramillo, R. Gomperts, R. E. Stratmann, O. Yazyev, A.J. Austin, R. Cammi, C. Pomelli, J.W. Ochterski, P. Y. Ayala, K. Morokuma, G.A. Voth, P. Salvador, J.J. Dannenberg, V.G. Zakrzewski, S. Dapprich, A.D. Daniels, M.C. Strain, O. Farkas, D.K. Malick, A.D. Rabuck, K. Raghavachari, J.B. Foresman, J.V. Ortiz, Q. Cui, A.G. Baboul, S. Clifford, J. Cioslowski, B.B. Stefanov, G. Liu, A. Liashenko, P. Piskorz, I. Komaromi, R. L. Martin, D.J. Fox, T. Keith, M.A. Al-Laham, C.Y. Peng, A. Nanayakkara, M. Challacombe, P.M.W. Gill, B. Johnson, W. Chen, M.W. Wong, C. Gonzalez, J. A. Pople, Gaussian 03, Revision C.02, Gaussian, Inc., Wallingford CT, 2004.

[29] F. Faglioni, P.S. D'Agostino, B. Cadioli, P. Lazzeretti, Parity violation energy of biomolecules–II: DNA, Chem. Phys. Lett. 407 (2005) 522–526, https://doi.org/10.1016/j.cplett.2005.04.009.

[30] C.J. Jameson, A.D. Dios, Absolute shielding scale for 31P from gas-phase NMR studies, Chem. Phys. Lett. 167 (1990) 575–582, https://doi.org/10.1016/0009-2614(90)85472-O.

[31] P. PyykkÖ, Spectroscopic nuclear quadrupole moments, Mol. Phys. 99 (2001) 1617–1629, https://doi.org/10.1080/00268970110069010.

[32] S. Adiga, D. Aebi, D.L. Bryce, EFGShield—A program for parsing and summarizing the results of electric field gradient and nuclear magnetic shielding tensor calculations, Can. J. Chem. 85 (2007) 496–505, https://doi.org/10.1139/v07-069.

[33] G. Mavel, NMR Studies of Phosphorus Compounds (1965–1969), Annual Reports on NMR Spectroscopy., 5B (1973) 1–305, https://doi.org/10.1016/S0066-4103(08)60357-9.

[34] J. Herzfeld, A.E. Berger, Sideband intensities in NMR spectra of samples spinning at the magic angle, J. Chem. Phys. 73 (1980) 6021–6030, https://doi.org/10.1063/1.440136.

[35] D.G. Gorenstein, D. Kar, 31P chemical shifts in phosphate diester monoanions. Bond angle and torsional angle effects, Biophys. Res. Commun. 65 (1975) 1073–1080, https://doi.org/10.1016/S0006291X(75)80495-5.

[36] F.G. Prado, C. Geissner-Prettre, B. Pullman, J.P. Daudy, Ab initio quantum mechanical calculations of the magnetic shielding tensor of phosphorus-31 of the phosphate group, J. Amer. Chem. Soc. 101 (1979) 1737–1742, https://doi.org/10.1021/ja00501a016.

[37] T.M. Alam, Influence of Basis Set on the Calculation of 31P Chemical Shifts, Report No. SAND98-2053, Sandia National Laboratories, Albuquerque, NM, 1998.

[38] S. Ganapathy, L. Delevoye, J.P. Amoureux, P.K. Madhu, Heteronuclear dipolar decoupling effects on multiple-quantum and satellite-transition magic-angle spinning NMR, Mag. Reson. Chem. 46 (2008) 948–954, https://doi.org/10.1002/mrc.2286.

[39] A. Goldbourt, P.K. Madhu, Multiple-quantum magic-angle spinning: High-resolution solid-state NMR of half-integer spin quadrupolar nuclei, Annual Reports of NMR Spectroscopy 54 (2004) 81–153, https://doi.org/10.1016/S0066-4103(04)54003-6.

[40] J. Trébosc, J.P. Amoureux, Z.H. Gan, Comparison of high-resolution solid-state NMR MQMAS and STMAS methods for half-integer quadrupolar nuclei, Solid. State. NMR. 31 (2007) 1–9, https://doi.org/10.1016/j.ssnmr.2006.09.002.

[41] M. Nausner, Jiří Brus, M. Häubl, N. Müller, W. Schoefberger, Characterization of the sodium binding sites in microcrystalline ATP by 23Na-solid-state NMR and ab initio calculations, Inorganica Chimica Acta 362 (2009) 1071–1077, https://doi.org/10.1016/j.ica.2008.05.030.

[42] A. Abragam, Principles of Nuclear Magnetic Resonance, Oxford University Press, Oxford, 1961, p. 261.